JOURNAL OF GEOPHYSICAL RESEARCH, VOL. 97, NO. B12, PAGES 17,615–17,625, NOVEMBER 10, 1992

Oblique Convergence and Deformation Along the Kuril and Japan Trenches

CHARLES DEMETS[1]

Jet Propulsion Laboratory, California Institute of Technology

The hypothesis that present-day deformation within the southern Kuril forearc is driven by oblique subduction of the Pacific plate is tested using 397 horizontal slip directions derived from shallow-thrust earthquakes from the Kuril and Japan trenches for the period 1963-1991. A simple two-plate model fits the 397 slip vectors significantly worse than a model that permits strike-slip motion of the southern Kuril forearc relative to the overlying plate. Weighted, mean slip directions along the southern Kuril trench are systematically rotated toward the direction orthogonal to the trench, which implies that the net convergence is partitioned into less oblique subduction and trench-parallel displacement of the southern Kuril forearc. The angular discrepancy between the observed slip direction and the direction predicted by the NUVEL-1 Pacific-North America Euler vector implies that the southern Kuril forearc translates 6–11 mm yr^{-1} to the southwest relative to the overlying North American plate. These results are consistent with geologically, geodetically, and seismologically observed convergence at the leading edge of the forearc sliver in southern Hokkaido and with previously inferred extension at the trailing edge of the sliver, which is located at the Bussol Strait at 46°N. The percentage of the oblique component of the rigid plate convergence vector that is transferred into forearc strike-slip motion is only 30%, which may be evidence that the Hokkaido/Honshu bend in the trench hinders southwest forearc motion or that the greater strength of oceanic forearcs impedes motion along forearc strike-slip faults.

INTRODUCTION

An increasing amount of evidence suggests that oblique convergence across a trench is accommodated through partitioning of slip into nearly orthogonal subduction along the main subduction thrust zone, and trench-parallel translation of forearc slivers along strike-slip faults. The evidence includes seismologic observations of strike-slip forearc earthquakes [e.g., *Fitch*, 1972; *Ekström and Engdahl*, 1989], marine seismic and bathymetric data that define strike-slip faults within the forearc [e.g., *Geist et al.*, 1988; *Ryan and Scholl*, 1989], and paleomagnetic observations of block rotations indicative of distributed trench-parallel shear [*Beck*, 1986; *Harbert*, 1987; *Beck*, 1989, 1991]. Studies of present-day plate velocities along trenches also support these observations. *Jarrard* [1986*a*, *b*] finds that along trenches where slip directions from shallow thrust earthquakes differ systematically from the rigid plate convergence direction predicted by the RM2 global plate motion model [*Minster and Jordan*, 1978], trench slip vectors are commonly rotated toward the trench-normal direction. *DeMets et al.* [1990] find a similar pattern using the more recent NUVEL-1 global plate motion model and an expanded set of trench earthquake slip vectors. The results of both of these studies suggest that where plates subduct at an angle that is oblique to the local trend of a trench, the trench-parallel component of the relative convergence vector can decouple forearc slivers from the rigid interior of the overlying plate and cause along-trench translation of the forearc slivers. In light of these results, it is apparent that models of the geological and tectonic evolution of plate margins adjacent to trenches require a better understanding of the relationships between oblique subduction, trench-parallel strike-slip displacements, and rotations of forearc slivers and blocks.

The purpose of this paper is to examine the relationship of oblique convergence across the Kuril and Japan trenches of the northwest Pacific basin to deformation of the southern Kuril forearc, the island of Hokkaido, and, to a lesser extent, the southern Kamchatka peninsula (Figure 1). The Kuril and Japan trenches are well suited to a study of oblique subduction for several reasons. First, the Kuril and Japan trenches do not describe a great circle and thus cannot accommodate orthogonal subduction everywhere. Second, numerous shallow-focus thrust earthquakes along these trenches have been modeled and can be used to estimate local directions of subduction. Finally, seismologic, geodetic, and geologic evidence for deformation within the forearc in Hokkaido and the Bussol Strait [*Seno*, 1985*a*; *Kimura*, 1986] can be used to validate kinematic models of forearc deformation.

Jarrard [1986*a*] presents evidence to support the hypothesis that motion of the southern Kuril forearc is driven by oblique subduction of the Pacific plate beneath the southern Kuril forearc. *Jarrard* [1986*a*] compares 63 horizontal earthquake slip vectors from the Kuril trench to the present-day convergence direction predicted by the RM2 Pacific-North America Euler vector and finds that 24 slip vectors from the southern Kuril trench (42.5°N-44.7°N) are oriented 7°±4° clockwise from the predicted rigid plate convergence direction. The sense and magnitude of the discrepancy suggests that the southern Kuril forearc translates 11±6 mm yr^{-1} to the southwest along the edge of the North American margin. The analysis presented here is similar to that of *Jarrard* [1986*a*] but with significant differences. First, many more shallow thrust earthquake slip vectors from the Kuril and Japan trenches are now available. The up-to-date compilation of earthquake focal mechanisms used here consists of 397 horizontal slip vectors from earthquakes that occurred between 1963 and April 1991. The sixfold increase in the number of slip vectors enables a more thorough determination of the

[1]Now at Department of Geology and Geophysics, University of Wisconsin at Madison, Madison, Wisconsin.

number 92JB01306.
0148-0227/92/92JB-01306$05.00

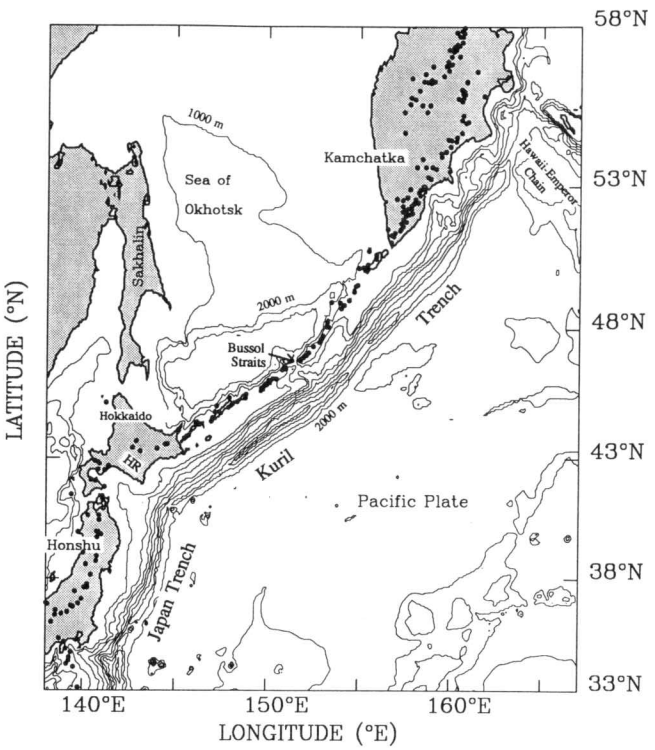

Fig. 1. Location map for features discussed in text. Bathymetry and all volcanoes with reported Quaternary activity (solid circles) are also shown (courtesy of Smithsonian Institution, Global Volcanism Program). HR is Hidaka Range. Bathymetric contour interval is 1000 m.

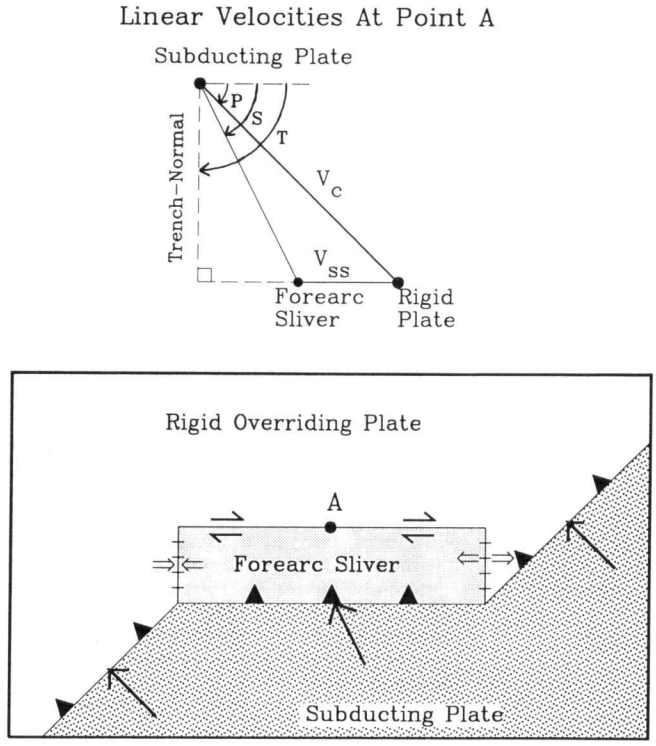

Fig. 2. (Top) Linear velocity vector diagram for the geometry in the lower half of the figure. V_C and P are the rate and direction of the predicted rigid plate velocity, which is oblique to the trench at point A. The mean subduction direction S is oriented between the trench-normal direction T and the rigid plate convergence direction P. (Bottom) Idealized subduction zone that accommodates normal and oblique convergence. Heavy arrows show the local direction of subduction beneath the forearc, as estimated from trench slip vectors ("S" in top figure). Where convergence is oblique, strike-slip motion occurs between the forearc and rigid, overriding plate. The zone of deformation along the boundaries of the sliver is likely to be wider than shown here.

mean subduction directions along the trench. Second, the RM2 global plate motion model used by *Jarrard* [1986*a*, *b*] is replaced with the newly published NUVEL-1 global plate motion model [*DeMets et al.*, 1990], which predicts convergence velocities across the Kuril and Japan trenches that are 10% slower than predicted by RM2. Finally, recent comparisons of alternative present-day plate configurations for northeast Asia and Japan suggest that the North American plate extends as far south as central Honshu island [*Seno*, 1985*b*; *DeMets*, 1992]. *DeMets* [1992] demonstrates that this geometry gives a good fit to slip vectors along the Japan trench and northern Kuril trench and satisfies the plate circuit closure constraints imposed by the NUVEL-1 model. These results thus provide a sound basis for this analysis.

The following questions are examined here. Can a single Euler (e.g., rotation) pole fit all 397 slip vectors from the Kuril and Japan trenches, which would be the case if the slip vectors recorded motion between only two plates? Are slip vectors from the southern Kuril trench oriented between the predicted Pacific-North America convergence direction and the direction normal to the trench, as observed by *Jarrard* [1986*a*]? How does the convergence obliquity, which is the angle between the Pacific-North America convergence direction and the trench-perpendicular direction, change along the trench (Figure 2), and how is the convergence obliquity partitioned between trench-parallel strike-slip motion and trench-normal convergence? Finally, how much forearc strike-slip motion is implied by the differences between the predicted convergence directions and the directions of subduction determined from trench slip vectors?

Estimating Forearc Strike-slip Rates Along Obliquely Convergent Margins

The observation that oblique convergence across a trench is often partitioned into less oblique subduction and trench-parallel translation and rotation of forearc slivers implies that horizontal slip directions estimated from shallow-thrust subduction zone earthquakes are rarely suitable for determining the convergence direction between major tectonic plates. Trench slip vectors instead provide valuable information about the direction of the subducting plate relative to the forearc sliver that is sandwiched between the subducting slab and the rigid interior of the overlying plate. The rate of strike-slip translation of a forearc sliver relative to the stable interior of the overlying plate can be inferred from the three-dimensional geometry of the subduction zone and from the local direction of subduction given by earthquake slip directions. The trench-parallel motion of the forearc V_{SS} is given by *McCaffrey* [1992] as

$$V_{SS} = \frac{V_C \sin(S - P)}{\cos(T - S)} \sqrt{\sin^2(T-P) + \cos^2(T-P)\cos^2 D} \quad (1)$$

where V_C, the rigid plate convergence rate, and P, the rigid

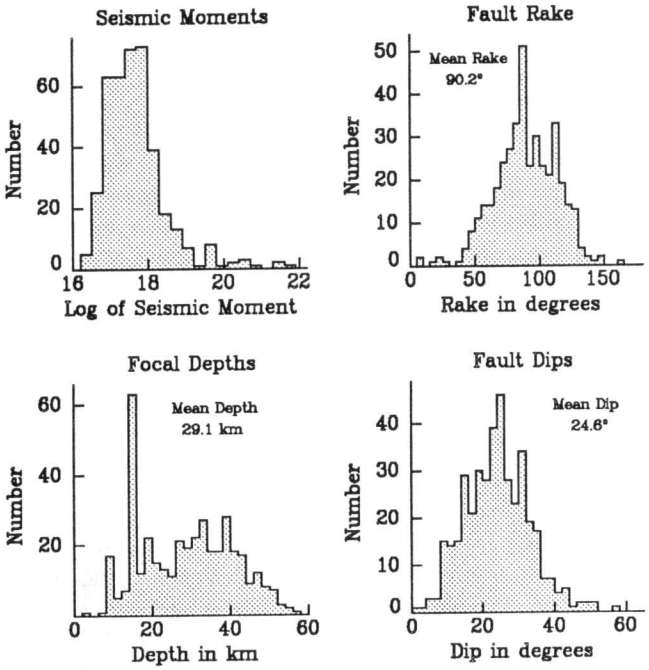

Fig. 3. Histograms of the seismic moments (units in Newton meters), fault dips, fault rakes (the direction of slip in the fault plane), and focal depths of the 397 shallow-thrust earthquakes along the Japan and Kuril trenches.

plate convergence direction, are predicted by the NUVEL-1 model, T, the trench-normal direction, is determined from measurements of the trend of the trench axis from bathymetric charts, S, the direction of subduction, is determined from the horizontal slip directions of shallow thrust earthquakes, and D, the dip of the subducting slab, is determined from measurements of the angle of the shallow Benioff zone. Equation (1) differs from the simpler two-dimensional formulation given by *Jarrard* [1986*a*] because of the necessity to compensate for dip of the subducting slab [*Beck*, 1991]. Prior to subduction, the motion of the subducting slab is horizontal; however, bending of the subducting slab during its descent beneath the forearc imparts a vertical component to the convergence velocity vector. Because only the horizontal component contributes to strike-slip motion along the forearc, the convergence velocity must be corrected through rotation to the horizontal about the trench axis [*McCaffrey*, 1992]. *Beck* [1991] also derives a relationship between V_{SS} and the above parameters; however, it differs from equation (1) in that V_C is corrected through projection of the predicted convergence velocity onto the horizontal. Both formulations were tested and gave nearly identical values of V_{SS} and its uncertainties, which is not surprising given that the difference between rotation and projection to the horizontal for shallow dip angles is small.

The uncertainties in the five quantities used to determine V_{SS} are estimated as follows. The uncertainties for V_C and P are determined from the NUVEL-1 model covariances. Uncertainties in D are based on a subjective estimate of the accuracy with which slab dip can be measured from vertical cross sections of shallow trench seismicity. Uncertainties in T are estimated from trench bathymetric charts, and uncertainties in S are conservatively estimated by doubling the standard error of the mean direction that is determined from groups of slip vectors.

Assuming that the uncertainties in the five observed quantities used to compute V_{SS} are uncorrelated, σ_{SS}, the uncertainty in V_{SS}, can be estimated through linear propagation of errors. From equation (1) and the partial derivatives with respect to V_C, S, P, T, and D

$$\sigma_{SS} = V_{SS}\left[\left[\left(\frac{\sigma_{VC}}{V_C}\right)^2 + \left(\sigma_S\,(\cot(S-P) - \tan(T-S))\right)^2 + \left(\sigma_P\left[\cot(S-P)+\frac{\sin(2T-2P)\sin^2 D}{2C^2}\right]\right)^2 + \left(\sigma_T\left[\tan(T-S) + \frac{\sin(2T-2P)\sin^2 D}{2C^2}\right]\right)^2 + \left[\frac{\sigma_D \sin(2D)\cos^2(T-P)}{2C^2}\right]^2\right]^{\frac{1}{2}} \quad (2)$$

where σ_{VC}, σ_S, σ_P, σ_T, and σ_D are the uncertainties in the predicted convergence rate, the subduction direction, the predicted rigid plate direction, the trench-normal direction, and the slab dip, respectively. For notational convenience,

$$C = \sqrt{\sin^2(T-P) + \cos^2(T-P)\cos^2 D}. \quad (3)$$

Data and Techniques

Earthquake Slip Directions Along the Kuril and Kamchatka Trenches

The direction of the subducting Pacific plate relative to the forearc has been estimated from horizontal slip directions derived from the focal mechanisms of shallow (i.e., above 50 km) thrust earthquakes. In order to compile as much information as possible about the subduction directions between 35.5°N, where the Izu trench intersects the southern Japan trench, and 54.0°N, where the northwestern end of the Hawaii-Emperor seamounts subduct beneath Kamchatka, the epicentral parameters for shallow-depth earthquakes for the period January 1963 to April 1991 were examined. A total of 397 earthquakes that appear to record slip along the subduction interface were identified, of which 293 were taken from the Harvard centroid moment tensor catalog (CMT). Most focal mechanisms for earthquakes that occurred before 1977 were taken from studies of the initial motions of P and S waves and S wave polarizations. Epicentral parameters, slip directions, and sources have been tabulated for each of the 397 earthquakes and are available upon request from the author.

As shown in Figure 3, a wide range of thrust focal mechanisms were considered acceptable for this analysis so as to avoid introducing any investigator bias into the data set. It was assumed that all thrust earthquakes down to a depth of 50 km record slip between the subducting and overlying plate; thus all thrust earthquakes with focal depths shallower than 50 km have been included, regardless of magnitude or the degree of dip-slip thrusting. Where possible, centroid depths were used because they are likely to be more accurate than preliminary depth estimates from the National Earthquake Information Service [*Dziewonski and Woodhouse*, 1983]. Twelve earthquakes with focal depths deeper than 50 km were

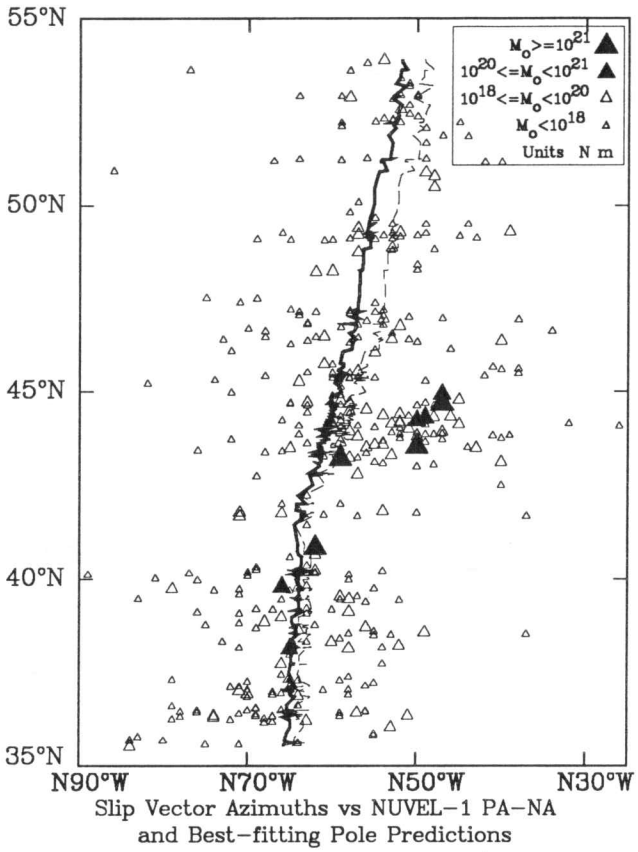

Fig. 4. Convergence directions predicted by the NUVEL-1 Pacific-North America Euler pole (solid line) and best fitting Euler pole (dashed line) and the 397 earthquake slip vectors (triangles). Slip vector averaging (Figure 5) helps to reduce the scatter in the individually observed slip vectors.

included because their focal mechanisms are consistent with subduction-related thrusting on a shallow-dipping fault plane. Earthquakes with fault planes that dip more than 60° were excluded so as to minimize the chances of including earthquakes that do not represent slip along the shallow subduction zone fault. Finally, two shallow thrust earthquakes (January 23, 1988 and June 21, 1988) were omitted because they have horizontal slip directions that differ by more than 45° (~3σ) from the mean directions determined from other nearby earthquakes.

Mean Subduction Directions Along the Trench

Following compilation of the 397 thrust focal mechanisms, the horizontal slip direction for each earthquake was computed by rotating the slip direction for the northwest dipping nodal plane to the horizontal in the manner described by *Minster and Jordan* [1978]. The along-trench slip vector distribution shows a 30°-35° variation for a given latitude (Figure 4), which tends to obscure the true subduction directions. To reduce this noise, slip directions were grouped together for every 2° of latitude north and south of the prominent bend in the trench at 41°N, and mean slip directions and uncertainties were computed (Table 1).

The determination of mean slip directions requires a method for weighting slip directions from individual earthquakes. Large earthquakes, which are typically detected by more seismic stations than are small earthquakes, have better constrained focal mechanisms and slip vectors than most small earthquakes. The assumed greater accuracy of slip vectors derived from large earthquakes has been factored into this analysis by assigning uncertainties of 15°, 20°, or 25°, depending on whether the seismic moment release is greater than 10^{18} N m, between 10^{17} and 10^{18} N m, or less than 10^{17} N m, respectively. These criteria are identical to the criteria used to assign slip vector uncertainties in the NUVEL-1 data set.

The adopted weighting scheme represents a relatively equitable use of slip directions determined from small and large earthquakes. Slip directions for large earthquakes are assigned at most 1.67 times the weight of slip directions for small earthquakes, which minimizes the chances that an error in the slip vector for a large subduction zone earthquake will significantly bias the estimated mean slip direction for a given trench segment. The principal disadvantage of the adopted weighting scheme is its failure to recognize that slip that occurs during the infrequent great subduction zone earthquakes dominates the long-term seismic moment release and should thus be weighted accordingly heavier. For instance, the seismic moment release for the largest earthquake in the data set (October 13, 1963) exceeds the moment release for the smallest earthquakes by 4 to 5 orders of magnitude. Although it would seem prudent to assign much more weight to the slip direction determined for a large earthquake, the mean slip directions for sections of the trench with large earthquakes would become overly sensitive to any errors in the focal mechanisms for these few earthquakes. Because geographic limitations in global and local seismic network configurations, and the perturbing effects of upper mantle structure on seismic wave propagation [*Engdahl et al.*, 1977; *Molnar and Chen*, 1982] limit how accurately an earthquake focal mechanism can be modeled, regardless of its magnitude, it is probably risky to assign relative slip vector weights based on seismic moment release. *Molnar and Chen* [1982] suggest that ±10° is the safe lower bound on the accuracy with which individual fault plane and nodal plane strikes can be modeled at present, regardless of the size of the earthquake. Because horizontal slip directions depend primarily on the strike of the auxiliary nodal plane, this suggests that the lowest individual slip vector uncertainty is also ~±10°.

Because of the difficulty in finding a weighting scheme that accounts for the amount of slip that occurs during an earthquake while also recognizing the limited accuracy of slip vectors determined for even the largest earthquakes, the mean slip directions determined from the above weighting scheme represent a compromise solution. To assess the degree to which the mean slip directions (and thus the conclusions of this analysis) depend on the adopted weighted scheme, two additional weighting schemes, namely, weighting by the seismic moment release and body wave magnitude of an earthquake were also investigated. The mean slip directions determined using these two weighting schemes were only 1°–3° different from those given in Table 1 with one exception; the moment-weighted slip direction for the latitudes 44°N–46°N is 7° clockwise (CW) from the mean direction given in Table 1. None of these difference are large enough to affect the results or conclusions of this study.

Two checks of the internal consistency of the 397 slip directions were also conducted. The first entailed comparison of slip directions determined from first-motion solutions to slip directions derived from the presumably more robust CMT solutions. On average, the 104 slip vectors determined from first-motion solutions are oriented 3° CW from the CMT slip

TABLE 1. Mean Slip Directions, Convergence Obliquities, and Rates of Forearc Strike Slip

Latitude Range	Number of Slip Vectors	Mean Slip Direction	Trench Normal	V_{plate}		Slab Dip†	Forearc Slip Rate	Sense of Slip
				Rate	Azimuth			
52°-54°N	27	-54.4°±2.2°	-58°±3°	78.7±1.5	-51.4°±0.9°	19°±2°	4±3	S
50°-52°N	15	-53.4°±6.0°	-58°±3°	81.3±1.5	-53.7°±0.9°	19°±2°	-	none
48°-50°N	32	-54.1°±2.3°	-49°±2°	82.5±1.5	-55.3°±0.9°	22°±2°	2±3	S
48°-46°N	42	-58.0°±3.0°	-49°±2°	83.8±1.5	-57.4°±0.9°	22°±2°	-	none
46°-44°N	78	-54.6°±2.1°	-36°±2°	84.8±1.4	-59.4°±0.9°	22°±2°	7±3	D
44°-42°N	53	-54.7°±2.4°	-36°±2°	85.9±1.4	-62.5°±0.9°	22°±2°	11±4	D
43°-41°N	18	-59.2°±4.8°	-36°±2°	86.2±1.4	-63.3°±0.9°	22°±2°	6±7	D
41°-39°N	47	-65.4°±2.4°	-79°±2°	86.6±1.4	-63.9°±0.9°	15°±2°	2±4	D
39°-37°N	45	-63.2°±2.9°	-79°±2°	86.9±1.4	-64.8°±0.8°	15°±2°	-	none
37°-35.5°N	48	-68.3°±2.7°	-65±2°	87.0±1.4	-65.4°±0.8°	15°±2°	-	none

Trench normal is the direction measured perpendicular to the local strike of the trench. V_{plate} is the Pacific-North America velocity predicted by the NUVEL-1 model at the midpoint of the trench segment. The rate of forearc strike-slip motion computed from these values and equation (1) is assumed to be parallel to the local trend of the trench. All rates are given in millimeters per year, and all directions are given in degrees clockwise from north. All uncertainties are 1σ. The sense of forearc slip is dextral (D) where the predicted plate direction is counterclockwise from the mean slip vector direction, and sinistral (S) for a clockwise discrepancy. A dash indicates that the trench slip vectors do not lie between the trench-normal and predicted convergence direction.

† Shallow slab dips are taken from *Jarrard* [1986*b*].

direction, with no systematic pattern along the trench. The mean direction determined from all 397 first-motion and CMT slip vectors differs from the mean direction determined solely from CMT solutions by only 0.8°. Given the small difference between the average slip directions determined from first-motion and CMT studies, there appears to be little reason to suspect a systematic problem with either data set. The second check entailed a search for systematic trends in earthquake slip directions as a function of distance perpendicular to the trench axis, as might be observed if the forearc undergoes distributed shear through slip along several subparallel forearc strike-slip faults. Ten trench-normal latitudinal bands were plotted as a function of distance from the trench axis, and the best fitting linear trend and uncertainty for each latitudinal band was computed. No significant trends were observed, which suggests that distributed forearc deformation that might cause systematic rotation of slip vectors as a function of distance from the trench axis either does not occur or is beneath the resolution of the slip vectors.

The Present-Day Pacific-North America Convergence Direction

As implied by equation (1), it is necessary to know the rigid plate convergence direction vector in order to determine whether convergence is oblique to the trench. *DeMets* [1992] demonstrates that the simplest plate geometry consistent with NUVEL-1 plate circuit closures and Kuril and Japan trench earthquake slip vectors is a geometry in which the rigid plate interior as far south as 41°N is part of the North American plate. This implies that the NUVEL-1 3.0 Ma-average Pacific-North America Euler vector [*DeMets et al.*, 1990] should be used to predict the rate and direction of rigid-plate convergence along the trench for comparison to the mean slip directions. The NUVEL-1 model is well suited to this analysis because it satisfies global plate circuit closure constraints, which guarantees that information from plate boundaries with high-quality data such as spreading rates and transform fault azimuths will propagate through the model and help to determine velocities along plate boundaries such as trenches where few reliable data exist. NUVEL-1 is also free from the significant biases in estimates of Pacific basin plate velocities that affected prior global plate motion models [*Chase*, 1978; *Minster and Jordan*, 1978].

There are two possible shortcomings to using NUVEL-1 to predict Pacific-North America motion. First, the 3.0-m.y. averaging interval for the NUVEL-1 model is far longer than the ~30-100 year strain averaging interval for major, shallow-thrust earthquakes along the Japan and Kuril trenches. If Pacific-North America motion has changed significantly over the past 3.0 m.y., the direction predicted by NUVEL-1 could differ in an unknown way from the instantaneous convergence direction that is appropriate for comparison to the trench slip vectors. Fortunately, this does not appear to be a problem. An analysis of 4 years of very long baseline interferometric (VLBI) measurements between sites located in the stable interiors of the North American and Pacific plates gives Pacific-North America velocities that differ by no more than 4±7 mm yr^{-1} and 3°±4° anywhere along their mutual boundary [*Argus and Gordon*, 1990]. This difference constitutes no more than 5% of the total convergence rate along the Kuril and Japan trenches.

The second possible shortcoming is that 15 of the northern Kuril trench slip vectors used here to provide a model-independent estimate of subduction directions along the trench were also used to derive NUVEL-1. The mean subduction directions *S* and the predicted convergence directions *P* are thus not independent along the northern Kuril trench. To test how this might affect the analysis, the 15 slip vectors were deleted from the 1122 data used to derive NUVEL-1 and the remaining 1107 data were inverted to derive a modified global plate motion model. The modified Pacific-North America Euler vector predicts velocities along the Kuril and Japan trenches less than 0.1° and 0.1 mm yr^{-1} different than predicted by NUVEL-1. Thus, for the purposes of this study, NUVEL-1 is considered to give an independent estimate of Pacific-North America velocities.

DEFORMATION OF THE KURIL FOREARC

Statistical Test for the Southern Kuril Sliver Plate

The main goal of this analysis is to determine what information the 397 slip vectors along the Kuril and Japan trenches

contain about deformation of the lithosphere that overlies the trench. To do so, three models that assume different near-trench plate geometries are analyzed in order to determine which model better fits the 397 slip vectors. The first model is a simple two-plate model in which the Pacific plate subducts beneath a single overlying plate. Because this model is derived solely from the 397 slip vectors, no assumptions about the regional plate geometry (such as whether the overlying plate is part of the North American or Eurasian plate) are necessary. The conclusions from this part of the analysis are thus independent from the larger-scale question of the proper regional plate geometry, which is considered in detail by *DeMets* [1992]. The second model incorporates three plates: the subducting Pacific plate, a major overlying plate, and a southern Kuril sliver plate, which is sandwiched between the trench and the major overriding plate from the Bussol Strait at 46.1°N to the Honshu/Hokkaido bend at 41°N. The third model further incorporates an unnamed forearc sliver located from 52°N to 54°N.

To test the simple model in which the Pacific plate subducts beneath a single, rigid overlying plate along the entire length of the Japan and Kuril trenches, the 397 slip directions are first compared to the directions predicted by an Euler pole that best fits the 397 slip vectors. If this model accurately describes the regional plate geometry, then the slip vectors should be well fit by a single best fitting Euler pole. To derive the best fitting Euler pole, the 397 slip vectors are inverted to determine the Euler pole that minimizes the least squares misfit. Visual comparison of the directions predicted by the best fitting pole, which is located at 15.7°N, 299.0°E, to the scattered slip vectors reveals little of consequence (Figure 4); however, a comparison to the mean slip directions determined from the 397 slip vectors (Table 1) is more illuminating. From 41°N to 46°N and from 52°N to 54°N, the mean slip directions are oriented between the direction perpendicular to the trench and the direction predicted by the best fitting Euler pole (Figure 5). The intermediate orientation of the earthquake slip vectors is consistent with the pattern observed along other trenches where oblique convergence induces along-arc translation of forearc slivers. It thus appears that a more complex plate geometry which incorporates at least one forearc sliver is warranted.

To test whether models that incorporate forearc slivers from 41°N to 46°N and from 52°N to 54°N fit the 397 slip vectors significantly better than a simpler two-plate model, a slightly modified form of the F ratio test for an additional plate [*Stein and Gordon*, 1984] is used to compare the weighted, least squares misfits of the three models. Because only slip directions are considered here, the modified F ratio test ignores the angular rotation rate, which is one of the three

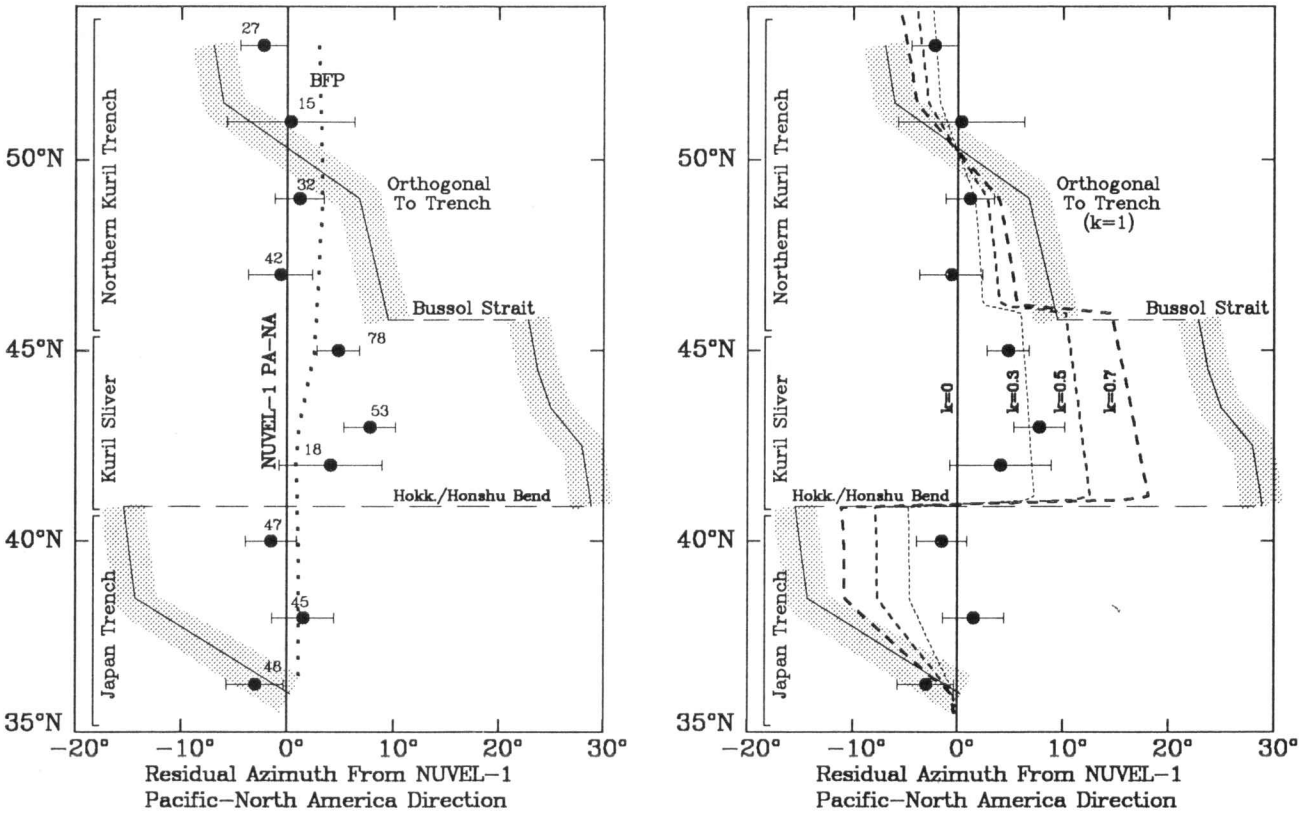

Fig. 5. (Left) Mean slip directions (circles) and 1σ uncertainties and trench-normal directions and uncertainties (shaded regions) shown as residual directions from the Pacific-North America convergence directions predicted by the NUVEL-1 model (vertical heavy line). The directions predicted by the rotation pole that best fits the 397 earthquake slip vectors (BFP; short-dashed line) shown in Figure 4 are also shown. The mean slip directions are well fit nearly everywhere except along the southern Kuril forearc between 41°N and 46°N. The small numbers above the mean slip directions are the number of individual slip vectors used to determine the mean directions. (Right) Mean slip directions compared to directions predicted by equation (4) for three different assumed values of slip partitioning. The mean slip directions are fit best when $k = 0.3$. Slip directions from the Japan trench suggest there is no partitioning, which implies that Pacific-North America motion is accommodated as oblique slip along the main subduction fault.

parameters required to specify a best fitting Euler vector. As a result, the F ratio test employs $(p\text{-}1)*2$ and $N\text{-}2p+2$ degrees of freedom, where p is the number of plates required by the geometry being tested, $2p\text{-}2$ represents the latitudes and longitudes required to specify the best fitting poles, and N is the number of earthquake slip vectors. The 99% reference value is adopted as the cutoff for a significant difference between the fits of two models.

For a two-plate model that best fits all 397 slip vectors, the total least squares misfit is $\chi^2 = 62.0$. For a three-plate model that consists of two best fitting Euler poles, one of which best fits the 141 slip vectors from 41°N to 46°N and the other of which best fits the remaining 256 slip vectors, $\chi^2 = 54.3$. Application of the *Stein and Gordon* [1984] F ratio test gives $F = 27.9$, which is much higher than the 99% reference value of $F = 4.7$. Thus the 397 slip vectors are significantly better fit by a model in which the southern Kuril forearc is detached from the overlying plate north of the Bussol Straits at 46°N and south of the Honshu/Hokkaido bend at 41°N.

For a four-plate model in which forearc slivers exist between 41°N and 46°N and between 52°N and 54°N, $\chi^2 = 54.0$, slightly lower than $\chi^2 = 54.3$ for the three-plate model. The small decrease in the misfit associated with an assumed forearc sliver between 52°N and 54°N is thus not statistically significant.

Given that the 141 slip vectors from the southern Kuril trench indicate that subduction is oblique along this segment of the trench, and that oblique subduction typically causes along-arc translation of forearc slivers, it is reasonable to conclude that oblique convergence along the southern Kuril forearc drives the geologically-observed southwestward motion of the southern Kuril forearc relative to the upper plate. In the following section, the 141 slip vectors along the southern Kuril trench are used in equation (1) to estimate the rate of implied forearc strike-slip motion.

Rate of Forearc Translation

Table 1 and equations (1) and (2) summarize the information needed to compute the rates of arc-parallel strike-slip motion and their uncertainties. Along the southern Kuril forearc, the angular discrepancy between the mean slip directions and predicted rigid plate direction is consistent with southwest directed, trench-parallel forearc translation of 6–11 mm yr^{-1} (Table 1). Of the three mean directions along the southern Kuril forearc, the mean direction for the 41°N-43°N trench segment is the least reliable. This section of the trench has fewer slip vectors than the two segments to the north and has not been ruptured by a recent major earthquake that could be used to estimate the local subduction direction. Given the realistic uncertainties in this analysis, the best estimate for the current arc-parallel motion of the southern Kuril sliver plate relative to North America is 6–11 mm yr^{-1}.

The slip vector discrepancy for the trench segment from 52°N to 54°N, which corresponds to subduction beneath southern and central Kamchatka, is consistent with 4±3 mm yr^{-1} (1σ) of left-lateral trench-parallel motion. For several reasons, it is unclear whether this result is reliable. First, the statistical analysis discussed above rejects a plate geometry that incorporates a forearc sliver located between 52°N and 54°N. Second, a major earthquake has not ruptured this section of the trench since the $M_W = 9.0$ earthquake ruptured a 650-km section of the trench in 1952. Finally, a survey of the literature uncovered no unambiguous geologic or seismologic evidence for sinistral slip along trench-parallel faults in central eastern Kamchatka. In light of these facts, no further speculation about this discrepancy seems warranted.

Discussion

Geologic, Geodetic, and Seismologic Evidence for Translation of the Southern Kuril Forearc

The first-order result of this analysis is the predicted southwestward translation of the southern Kuril forearc sliver, and the corollary deformation at the leading and trailing edges of the sliver. Much independent evidence supports this result [*Seno*, 1985*a*; *Kimura*, 1986]. The observational evidence includes the following: (1) Islands in the southern Kuril forearc and accreted forearc structures on the island of Hokkaido have en echelon orientations that are consistent with dextral strike-slip motion of the forearc [*Kaizuka*, 1975]. (2) Along the leading edge of the Kuril forearc sliver in southern Hokkaido, trench-parallel thrusting occurs along faults that strike nearly perpendicular to the trench (Figure 6) [*Kimura*, 1986]. (3) Strike-slip and thrust faulting associated with uplift of the Hidaka Mountains of southern Hokkaido indicate that the principal stress responsible for uplift at the leading edge of the sliver is oriented parallel to the trench [*Seno*, 1985*a*]. (4) Triangulation and trilateration measurements of displacements that occurred between 1896 and 1984 within extensive geodetic networks on Hokkaido show the southwestward displacements in northeastern Hokkaido that are associated with southwest migration of the forearc [*Hashimoto and Tada*, 1987; *Tada and Kimura*, 1987].

Because the forearc northeast of Hokkaido is largely underwater, it is more difficult to document evidence for forearc translation in this region. Nonetheless, there appears to be some evidence that the forearc is detached from the rigid overlying plate. Near the Bussol Strait at 46.1°N, a 5000-m-deep trough transecting the forearc appears to be an active graben that accommodates arc-parallel extension along the trailing edge of the southern Kuril forearc sliver [*Kimura*, 1986]. A detailed marine geophysical survey of the southern Kuril forearc further reveals submarine faults that might accommodate southwestward translation of a forearc sliver [*Le Pichon et al.*, 1984].

To assess whether additional information about translation of the forearc can be gained from an examination of shallow near-trench seismicity, 39 focal mechanisms that appear to record deformation other than slip along the main subduction fault have been compiled from the literature and centroid moment tensor catalog (Table 2 and Figure 6). The author's interpretation of the tectonic significance of the 39 earthquakes should be considered speculative for several reasons. First, a typical subduction zone is characterized by a juxtaposition of fault types and stress regimes, and it is thus likely that only some of the 39 earthquakes give information about forearc deformation. The tectonic significance of a given earthquake is also often ambiguous because uncertainties in the epicentral parameters make it difficult to determine whether the earthquake occurred within the subducting or upper plate.

Earthquakes 32-36, which occurred at the leading edge of the southern Kuril forearc, offer the clearest evidence for southwestward translation of the southern Kuril forearc. Each of the five earthquakes is consistent with thrust motion along fault planes that strike nearly orthogonal to the nearby trench

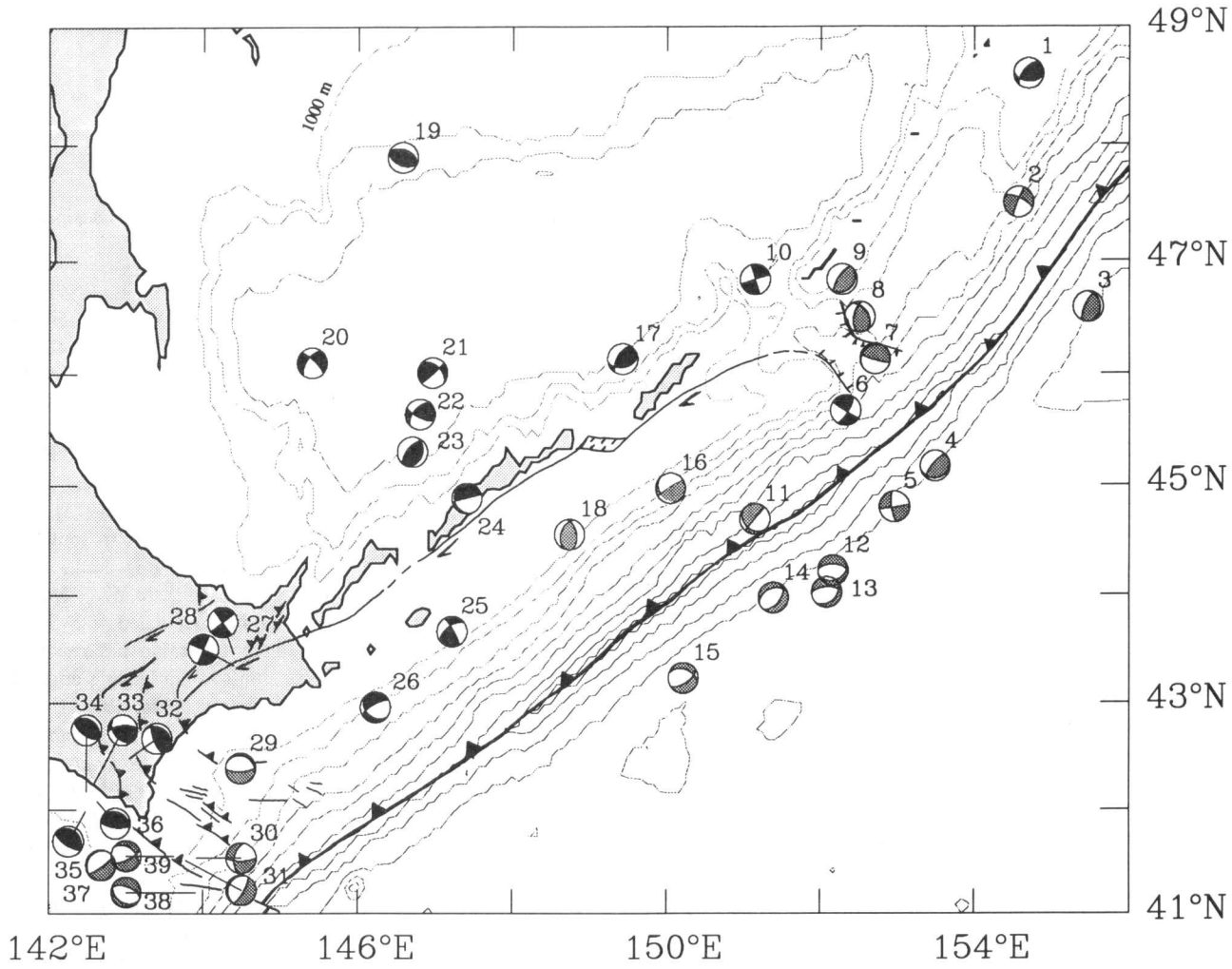

Fig. 6. Bathymetry and nonsubduction earthquakes in the vicinity of the southern Kuril forearc sliver. Epicentral parameters are given in Table 2. All published focal mechanisms for shallow nonthrust earthquakes are shown. Focal mechanisms with solid quadrants are believed to have occurred within the upper plate. Focal mechanisms with graytone quadrants record deformation with a less certain origin. Bathymetric contour intervals are 1000 m. All fault locations are taken from *Le Pichon et al.* [1984] and *Kimura* [1986].

[*Suzuki et al.*, 1983; *Seno*, 1985*a*]. The enhanced seismicity in this region offers evidence for the ongoing uplift of the Hidaka range of eastern Hokkaido [*Kimura*, 1986] in the collision zone at the leading edge of the forearc sliver.

Earthquakes 6 and 24-28 are all consistent with the predicted trench-parallel, dextral strike-slip motion within the forearc. In particular, earthquakes 24, 27, and 28 appear to support the hypothesis that some strike-slip motion occurs along faults located well inboard of the trench axis. Earthquakes 6, 25, and 26 are located closer to the trench axis, and if they are located within the forearc, they may indicate that the shear induced by oblique subduction is distributed along two or more subparallel strike-slip faults in the forearc.

The remaining earthquakes appear to have little relation to deformation of the forearc. Seismicity along the Bussol Strait (earthquakes 7-9), where forearc extension is predicted, is instead indicative of crustal shortening. A similar, but opposite anomaly is observed at the Honshu/Hokkaido bend in the trench at 41°N, where extensional earthquakes occur directly beneath the region where trench-parallel shortening is predicted to occur within the overlying plate. *Kanamori* [1971] postulates that the extensional earthquakes beneath the Honshu/Hokkaido bend record deformation of the Pacific plate as it is forced to subduct beneath the convexly-shaped forearc. Similarly, earthquakes 7-9 may represent bending of the Pacific plate as it subducts beneath the concavely-shaped bend at 46°N.

Finally, earthquakes 12-15 record flexing of the outer arc bulge of the Pacific plate prior to subduction, and earthquakes 1, 10, 17, and 19-23 all occur well northwest of the forearc and presumably record distributed deformation of the overlying plate. Earthquakes 2-5, 11, 16, 18, and 30 are anomalous and may have any number of explanations, including erroneous epicentral parameters.

Nonunique Nature of the Model

Although the model for forearc deformation discussed above provides useful constraints on forearc deformation rates, it is important to remember that the model is both nonunique and simplistic. For instance, strike-slip motion may occur along more than one fault in the forearc, as appears to be the case in the Aleutian forearc [*Ryan and Scholl*, 1989]. As discussed above, there is no evidence for systematic rotation of

TABLE 2. Epicentral Data and Source Parameters for Nonsubduction Earthquakes – Southern Kuril Region

Number in Figure	Date	Time, UT	Latitude[a] °N	Longitude[a] °E	Depth[b], km	M_o, N m	Mechanism[c]	Source
1	May 22, 1963	1356:43.0	48.60	154.70	22	3.0×10^{18}	95/45/135	SM
2	Nov. 17, 1984	1020:59.6	47.50	154.57	42	4.5×10^{17}	294/74/-168	CMT
3	Sept. 10, 1990	0351:24.2	46.59	155.48	38	9.8×10^{16}	354/22/60	D2
4	Aug. 2, 1983	0608:08.2	45.17	153.48	35	1.8×10^{17}	77/20/125	CMT
5	Sept. 17, 1988	1523:53.0	44.80	152.95	24	9.8×10^{16}	172/74/-177	CMT
6	April 08, 1981	2342:47.9	45.67	152.32	15	2.2×10^{17}	31/75/176	CMT
7	Oct. 14, 1984	0318:31.5	46.13	152.70	28	2.1×10^{17}	230/13/34	CMT
8	June 04, 1966	2348:17.8	46.50	152.50	27	9.0×10^{17}	191/57/118	SM
9	Jan. 10, 1978	0050:17.1	46.83	152.27	41	4.4×10^{17}	49/22/104	CMT
10	Jan. 2, 1975	not given	46.83	151.15	05	4.0×10^{18}	343/89/01	Sav83
11	June 30, 1982	0157:34.3	44.69	151.15	26	5.8×10^{19}	128/28/-03	CMT
12	April 21, 1988	1827:57.5	44.22	152.16	26	7.1×10^{16}	72/35/106	CMT
13	Feb. 10, 1980	1241:50.8	44.02	152.08	15	2.1×10^{17}	46/35/-125	CMT
14	Oct. 2, 1985	0316:27.2	43.97	151.39	18	5.3×10^{16}	248/40/-67	CMT
15	April 30, 1981	1441:41.2	43.23	150.22	11	3.1×10^{18}	288/42/-48	CMT
16	Aug. 21, 1988	1144:24.4	44.97	150.05	15	1.8×10^{17}	136/26/166	CMT
17	Jan. 14, 1985	0236:31.2	46.13	149.42	12	7.4×10^{16}	80/44/131	CMT
18	Jan. 29, 1989	1734:48.9	44.55	148.74	38	4.4×10^{16}	199/42/112	CMT
19	Nov. 15, 1978	0747:22.0	47.89	146.57	15	9.0×10^{17}	291/45/89	CMT
20	July 21, 1974	not given	46.10	145.40	30	2.0×10^{17}	214/60/-19	Sav83
21	July 1, 1964	0247:33.9	46.01	146.96	20	7.0×10^{17}	48/84/45	Sav83
22	July 25, 1968	1050:31.5	45.64	146.80	19	1.0×10^{19}	221/52/22	Sav83
23	May 7, 1962	1739:50.0	45.30	146.70	25	5.0×10^{19}	20/32/73	CS
24	Nov. 9, 1988	2329:54.5	44.88[d]	147.41[d]	15	8.2×10^{16}	162/20/-4	CMT
25	March 23, 1990	2106:03.7	43.66[e]	147.22[e]	20	1.1×10^{17}	234/59/168	D1
26	Nov. 23, 1981	1017:23.5	42.96	146.23	24	1.0×10^{18}	129/37/-27	CMT
27	Jan. 30, 1959	2216:00.0	43.45	144.40	20	5.0×10^{18}	53/89/179	Ich
28	Jan. 30, 1959	2038:00.0	43.35	144.40	10	6.0×10^{18}	23/89/179	Ich
29	Nov. 27, 1986	0328:58.5	42.39	144.49	35	6.6×10^{16}	294/18/-65	CMT
30	Jan. 19, 1979	1156:15.0	41.54	143.92	15	1.3×10^{17}	191/53/-161	CMT
31	April 30, 1983	1403:49.7	41.52	143.78	32	3.4×10^{18}	200/14/-99	CMT
32	Jan. 20, 1970	1733:03.1	42.48	143.04	25	2.0×10^{19}	300/24/54	CS
33	March 21, 1982	1022:33.2	42.26	142.59	37	2.1×10^{17}	141/41/139	CMT
34	March 21, 1982	0232:06.3	42.17	142.48	17	2.6×10^{19}	308/28/93	CMT
35	March 26, 1982	0155:02.0	41.99	142.47	15	1.2×10^{17}	316/23/101	CMT
36	May 22, 1982	0135:36.9	42.08	142.62	29	8.4×10^{16}	294/24/106	CMT
37	May 16, 1968	1039:01.6	41.47	142.67	33	3.6×10^{20}	54/81/-84	K71
38	Oct. 18, 1978	2330:20.2	41.21	143.91	15	1.6×10^{17}	123/32/-79	CMT
39	June 25, 1987	0327:06.1	41.56	143.63	15	5.4×10^{16}	307/40/-35	CMT

Sources are as follows. "CMT" is Harvard centroid moment-tensor solutions (see *Dziewonski et al.* [1990] for a complete listing of the references for the 1977-1989 solutions). References for post-1989 CMT solutions are D1, *Dziewonski et al.* [1991*a*] and D2, *Dziewonski et al.* [1991*b*]. Other souces are CS, *Chapman and Solomon* [1976]; Ich, *Ichikawa* [1971]; K71, *Kanamori* [1971]; SM, *Stauder and Mualchin* [1976]; and Sav83, *Savostin et al.* [1983].

a National Earthquake Information Service (NEIS) epicentral coordinates are used except where noted.

b All CMT focal depths are centroid depths.

c Strike (degrees clockwise from north)/dip (degrees clockwise about strike)/slip (degrees counterclockwise from strike, in nodal plane)

d Centroid epicentral coordinates. NEIS epicenter at 44.24°N, 148.32°E

e Centroid epicentral coordinates. NEIS epicenter at 43.76°N, 147.70°E

trench slip vectors as a function of distance from the trench axis, as might be expected for shear that is distributed across the forearc. Therefore the data do not require this additional level of model complexity. Finally, there is no requirement that translation of the forearc be directed parallel to the trench, as is assumed here. Computation of forearc translation rates for faults that are not parallel to the trench requires simple geometric adjustment of the computed trench-parallel rates (see Figure 2).

Slip Partitioning Along the Kuril and Japan Trenches

Slip partitioning is used to describe how much of the convergence obliquity is transferred to the forearc sliver and occurs as trench-parallel translation of the forearc. When partitioning is complete, all of the trench-parallel component of a rigid plate convergence velocity vector is transferred into strike-slip motion within the forearc, in which case the earthquake slip vectors will be oriented normal to the local trend of the trench. When no partitioning occurs, oblique convergence is accommodated entirely by oblique slip along the main subduction fault beneath the forearc, in which case trench slip vectors parallel the predicted convergence direction.

Neither of these end-member cases are typically observed. For reasons that are still unclear, partitioning instead varies widely between subduction zones. If slip partitioning is determined in part by the strength of the upper plate [*Jarrard*, 1986*b*], then oceanic forearcs, which are probably stronger than continental forearcs, should exhibit a lower degree of partitioning. *Beck* [1991] and *McCaffrey* [1992] further suggest that a minimum angle of obliquity must be exceeded before resistance to slip along a forearc fault is overcome, which implies that for low angles of obliquity, no partitioning may occur. *Beck* [1991] discusses another variable that could hinder motion of a forearc sliver and thus affect partitioning, namely, irregularities in the trace of a subduction zone. For instance, when a forearc sliver encounters a convex bend in

the trench, motion of the sliver must overcome the frictional and gravitational resistance required to thicken the crust at the leading edge of the sliver or within the sliver itself. An important unanswered question is whether the energy that an obliquely subducting slab imparts to a forearc sliver is less than, equal to, or greatly exceeds the energy required to overcome this resistance.

A reliable method for estimating slip partitioning, and ultimately, the ratio of resistance to slip along a forearc fault as opposed to slip along a subduction thrust is through comparison of trench slip vectors to trench-normal directions and the net convergence direction, as is done here. Slip partitioning for the Kuril and Japan trenches is computed using

$$S = T - \tan^{-1}\left[(1-k)\tan(T-P)\right] \quad (4)$$

where $k = V_{SS} / (V_C C \sin(T-P))$. Equation (4) is modified from the equation given by *Ekström and Engdahl* [1989] so as to use the same variables as in equations (1)-(3). When partitioning is complete, k=1; when no partitioning occurs, k=0 (Figure 5). Thus k is a simple measure of the efficiency with which the total amount of available oblique slip $V_C C \sin(T-P)$ is transferred into forearc strike-slip motion.

For values of k equal to 0.3, 0.5, and 0.7, the best fit to the mean slip directions occurs for k≈0.3 (Figure 5). Thus only about 30% of the component of the rigid plate convergence vector that is oriented parallel to the forearc is actually transferred to the forearc as strike-slip motion, while the remainder of the trench-parallel component is accommodated by slip along the subduction zone interface. It is unclear whether partitioning is low because of buttressing of the forearc sliver at the Honshu/Hokkaido corner, high resistance to slip along the strike-slip faults within the oceanic forearc, or another undetermined effect.

Interestingly, the data imply that slip partitioning does not occur along the Japan trench south of 41°N, even though the predicted rigid plate direction is up to 15° oblique to the trend of the trench (Figure 5). Two explanations for this apparent discrepancy are advanced. First, the assumption that northern Honshu and southern Hokkaido are part of the North American plate may be incorrect, and the good agreement between the mean slip directions (S) and the convergence direction predicted by the NUVEL-1 Pacific-North America Euler vector may be fortuitous. Although a model in which northern Honshu and southern Hokkaido move slowly relative to North America is more complex than required by the regional kinematic data [see *DeMets*, 1992], future geodetic and seismologic observations may warrant more complex models. A second plausible explanation is that convergence is not oblique enough to produce present-day strike-slip motion in Honshu. Unfortunately, there is no independent method with which to estimate the minimum angle of obliquity that is required to initiate strike-slip faulting in Honshu. A convincing explanation for this apparent anomaly thus appears beyond the reach of presently available data.

Future Work

Slip directions determined from future M = 8 shallow-thrust earthquakes should provide valuable additional information about trench slip directions that can be used to test the results of this analysis. Only four of the 22 major shallow earthquakes that have ruptured the Kuril and Japan subduction zones in the past century have occurred since 1963 [*Seno and Eguchi*, 1983]. The mean subduction directions along most of the trench are therefore estimated from small earthquakes. Although the mean slip directions that are derived from small subduction zone earthquakes appear to be similar to those determined from the larger earthquakes, the availability of more slip directions from well-constrained focal mechanisms of future large earthquakes would lend more credence to these results.

The principal result of this work, namely, that oblique subduction drives a sliver of the southern Kuril forearc at a rate of ~6–11 mm yr^{-1} relative to the adjacent North American plate, could be tested with geodetic measurements of site displacements in northeastern Hokkaido in a fixed North America reference frame. Annual measurements with the Global Positioning System receivers should be able to detect the predicted shortening within 1-3 years, assuming a well-executed network design and data analysis. Measurements to sites in the Kuril Islands would probably not measure the full predicted rate of shortening because the strike-slip faults that accommodate forearc slip appear to lie to the east of the islands [*Kimura*, 1986].

Acknowledgments. I thank Myrl Beck, Eric Geist, Rob McCaffrey, and Holly Ryan for comments that contributed to significant improvements in the manuscript. The writing and publication of this work was supported by the Jet Propulsion Laboratory, California Institute of Technology, under a contract with NASA. Reference herein to any specific commercial product, process, or service by trade name, trademark, manufacturer, or otherwise does not constitute or imply its endorsement by the United States government or the Jet Propulsion Laboratory, California Institute of Technology. This research was initially supported by a National Research Council fellowship at the Naval Research Laboratory.

References

Argus, D. F., and R. G. Gordon, Comparison of Pacific–North America plate motion determined from very long baseline radio interferometry with that determined from magnetic anomalies, transform faults, and earthquake slip vectors, *J. Geophys. Res., 95,* 17,315–17,324, 1990.

Beck, M. E., Model for late Mesozoic-Early Tertiary tectonics of coastal California and western Mexico and speculations on the origin of the San Andreas fault, *Tectonics, 5,* 49–64, 1986.

Beck, M. E., Block rotations in continental crust: Examples from western North America, in *Paleomagnetic Rotations and Continental Deformation,* edited by C. Kissel and C. Laj, pp. 1–16, Kluwer Academic, Boston, Mass., 1989.

Beck, M. E., Coastwise transport reconsidered: Lateral displacements in oblique subduction zones, and tectonic consequences, *Phys. Earth Planet. Inter., 68,* 1–8, 1991.

Chapman, M. E., and S. C. Solomon, North American–Eurasian plate boundary in Northeast Asia, *J. Geophys. Res., 81,* 921–930, 1976.

Chase, C. G., Plate kinematics: The Americas, East Africa, and the rest of the world, *Earth Planet. Sci. Lett., 37,* 355–368, 1978.

DeMets, C., A test of present-day plate geometries for northeast Asia and Japan, *J. Geophys. Res.,* in press, 1992.

DeMets, C., R. G. Gordon, D. F. Argus, and S. Stein, Current plate motions, *Geophys. J. Int., 101,* 425–478, 1990.

Dziewonski, A. M., and J. H. Woodhouse, An experiment in systematic study of global seismicity: Centroid-moment tensor solutions for 201 moderate and large earthquakes of 1981, *J. Geophys. Res., 88,* 3247–3271, 1983.

Dziewonski, A. M., G. Ekström, J. H. Woodhouse, and G. Zwart, Centroid-moment tensor solutions for October-December 1989, *Phys. Earth Planet. Inter., 62,* 194–207, 1990.

Dziewonski, A. M., G. Ekström, J. H. Woodhouse, and G. Zwart, Centroid-moment tensor solutions for January-March 1990, *Phys. Earth Planet. Inter., 65,* 197–206, 1991*a*.

Dziewonski, A. M., G. Ekström, J. H. Woodhouse, and G. Zwart,

Centroid-moment tensor solutions for July-September 1990, *Phys. Earth Planet. Inter., 67,* 211–220, 1991*b*.

Ekström, G., and E. R. Engdahl, Earthquake source parameters and stress distribution in the Adak Island region of the Central Aleutian Islands, Alaska, *J. Geophys. Res., 94,* 15,499–15,519, 1989.

Engdahl, E. R., N. H. Sleep, and M. T. Lin, Plate effects in North Pacific subduction zones, *Tectonophysics, 37,* 95–116, 1977.

Fitch, T. J., Plate convergence, transcurrent faults, and internal deformation adjacent to Southeast Asia and the western Pacific, *J. Geophys. Res., 77,* 4432–4460, 1972.

Geist, E. L., J. R. Childs, and D. W. Scholl, The origin of summit basins of the Aleutian Ridge: Implications for block rotation of an arc massif, *Tectonics, 7,* 327–341, 1988.

Harbert, W. P., New paleomagnetic data from the Aleutian islands: Implications for terrane migration and deposition of the Zodiac fan, *Tectonics, 6,* 585–602, 1987.

Hashimoto, M., and T. Tada, Horizontal crustal movements in Hokkaido and its tectonic implications, *Zishin, 41,* 29–38, 1988.

Ichikawa, M., Reanalyses of mechanisms of earthquakes which occurred in and near Japan, and statistical studies on the nodal plane solutions obtained, 1926-1968, *Geophys. Mag., 35,* 207–274, 1971.

Jarrard, R. D., Relations among subduction parameters, *Rev. Geophys., 24,* 217–284, 1986*a*.

Jarrard, R. D., Terrane motion by strike-slip faulting of forearc slivers, *Geology, 14,* 780–783, 1986*b*.

Kaizuka, S., A tectonic model for the morphology of arc-trench systems, especially for the echelon ridges and mid-arc faults, *Jpn. J. Geol. Geogr., 45,* 9–28, 1975.

Kanamori, H., Focal mechanism of the Tokachi-Oki earthquake of May 16, 1968: Contortion of the lithosphere at a junction of two trenches, *Tectonophysics, 12,* 1–13, 1971.

Kimura, G., Oblique subduction and collision: Forearc tectonics of the Kuril arc, *Geology, 14,* 404–407, 1986.

Le Pichon, X., T. Iiyama, V. Renard, K. Nakamura, J. Cadet, and K. Kobayashi, Phase 1 of the French-Japanese cooperative research "KAIKO" Project and its results, *Tokyo J. Earth Sci., 93,* 30–42, 1984.

McCaffrey, R., Oblique plate convergence, slip vectors, and forearc deformation, *J. Geophys. Res., 97,* 8905–8915, 1992.

Minster, J. B., and T. H. Jordan, Present-day plate motions, *J. Geophys. Res., 83,* 5331–5354, 1978.

Molnar, P., and W. P. Chen, Seismicity and Mountain Building, in *Mountain Building Processes,* edited by K. J. Hsü, pp. 1–57, Academic, San Diego, Calif., 1982.

Ryan, H. F., and D. W. Scholl, The evolution of forearc structures along an oblique convergent margin, central Aleutian arc, *Tectonics, 8,* 497–516, 1989.

Savostin, L., L. Zonenshain, and B. Baranov, Geology and plate tectonics of the Sea of Okhotsk, in *Geodynamics of the Western Pacific–Indonesian Region, Geodyn. Ser.,* vol. 11, edited by T. W. C. Hilde and S. Uyeda, pp. 189–222, AGU, 1983.

Seno, T., "Northern Honshu microplate" hypothesis and tectonics in the surrounding region, *J. Geod. Soc. Jpn., 31,* 106–123, 1985*a*.

Seno, T., Is northern Honshu a microplate?, *Tectonophysics, 115,* 177–196, 1985*b*.

Seno, T., and T. Eguchi, Seismotectonics of the western Pacific region, in *Geodynamics of the Western Pacific–Indonesian Region, Geodyn. Ser.,* vol. 11, edited by T. W. C. Hilde and S. Uyeda, pp. 5–40, AGU, Washington, D.C., 1983.

Stauder, W., and L. Mualchin, Fault motion in the larger earthquakes of the Kurile-Kamchatka arc and of the Kurile-Hokkaido corner, *J. Geophys. Res., 81,* 297–308, 1976.

Stein, S., and R. G. Gordon, Statistical tests of additional plate boundaries from plate motion inversions, *Earth Planet. Sci. Lett., 69,* 401–412, 1984.

Suzuki, S., Y. Motoya, N. Umino, A. Hasegawa, S. Kameya, and K. Tanaka, Hypocentral distribution and composite focal mechanisms of shallow earthquakes near the junction between the Kurile and the northeastern Japan arcs, *Zishin, 36,* 407–421, 1983.

Tada, T., and G. Kimura, Collision tectonics and crustal deformation at the southwestern margin of the Kuril arc, *Zishin, 40,* 197–204, 1987.

C. DeMets, Department of Geology and Geophysics, University of Wisconsin at Madison, 1215 W Dayton St., Madison, WI 53706.

(Received January 10, 1992;
revised May 29, 1992;
accepted June 3, 1992.)